Experimental demonstration of an adaptive orthogonal frequency division multiplexing visible light communication system

Xinyue Guo (郭心悦)* and Xin Li (李 鑫)

Shanghai Key Lab of Modern Optical Systems, School of Optical-Electrical and Computing Engineering, University of Shanghai for Science and Technology, Shanghai 200093, China

**Corresponding author: guoxinyue21@163.com*

Received July 17, 2016; accepted September 23, 2016; posted online October 26, 2016

We propose and experimentally demonstrate a simple visible light communication system by combining an adaptive transmission technique with orthogonal frequency division multiplexing. In the adaptive transmission scheme, power allocation is performed in such a way as to maximize the channel capacity under electric power constraints, and adaptive modulation is then introduced to achieve the maximum data rate given a target bit error rate. Experimental results show that spectrum efficiency can be greatly improved through this adaptive transmission technique.

OCIS codes: 060.2605, 060.4080.

doi: 10.3788/COL201614.110604.

Recently, visible light communication (VLC) based on white light-emitting diodes (LEDs) is garnering increasing attention in both academia and industry[1–4]. With the benefits of being cost effective, license free, electromagnetic interference free, and highly secure, it is one of the most compelling technologies for supplementing traditional radio frequency communication, especially in areas such as hospital, aircraft, and high-security environments[5,6]; however, the data rate of the VLC link is limited by the modulation bandwidth of the high-brightness LEDs used in light fixtures and lamps. Due to the power–bandwidth trade-off of LEDs and various parasitic impedances in the LED packaging, signals modulated at high frequencies are strongly attenuated[2]. As a result, the frequency response of the LED is not flat, which causes serious intersymbol interference (ISI) for high-speed transmissions. The orthogonal frequency division multiplexing (OFDM) scheme has been proposed to improve the data rate, and has proved particularly convenient for VLC systems because it decomposes the channel into multiple parallel frequency-flat subchannels to eliminate ISI[7–10].

Adaptive transmission techniques have also been recently introduced to improve spectrum efficiency. Wu *et al.* provide an in-depth theoretical analysis of adaptive modulation for high-speed VLC[11]. Park *et al.* propose a VLC transmission power optimization scheme that minimizes the bit error rate (BER)[12]. A framework for transmission power and rate optimization is built under certain lighting constraints in Ref. [13]. All these works prove that high data rates can theoretically be achieved over such limited bandwidths by using adaptive transmission techniques; however, adaptive VLC system design and the experimental demonstration are not referenced. Chow *et al.* propose and demonstrate an adaptive control of the OFDM modulation order to maintain the VLC transmission performance[14], where the modulation order is adapted according to the received signal-to-noise ratio (SNR) and the same modulation order is used in all the subcarriers. Afterward, Yeh *et al.* provide an adaptive OFDM scheme where the bit loading is introduced to obtain the optimal SNR of each subcarrier[15]. Both schemes are practical and the system performance can be greatly improved; however, the maximum spectrum efficiency is not achieved.

In this Letter, we propose and experimentally demonstrate a simple VLC system by combining an adaptive transmission technique with OFDM. A realizable adaptive transmission technique is proposed for an OFDM-based VLC system that is aimed at spectrum efficiency maximization under the constraints of power and the target BER. The adaptive OFDM scheme is implemented by two steps. The first step is power allocation. Power is allocated to each frequency-flat subchannel based on the idea of maximizing the channel capacity under electric power constraints. The second step is adaptive modulation. Maximum spectrum efficiency under certain BER constraints is achieved by adaptive modulation. Different modulation orders are determined for each subchannel according to a target BER and SNR. Then an experimental demonstration is set up to verify the effectiveness of the proposed adaptive VLC system. Experimental results show that the adaptive transmission scheme can greatly improve the spectrum efficiency as compared to the system without adaptive transmission.

A block diagram of the OFDM-based VLC system using the adaptive transmission technique is presented in Fig. 1. In the system, OFDM modulation is employed to eliminate the ISI and increase the data rate. An adaptive transmission scheme containing power allocation, adaptive modulation, and power control is proposed to increase the data rate further.

 © 2016 Chinese Optics Letters

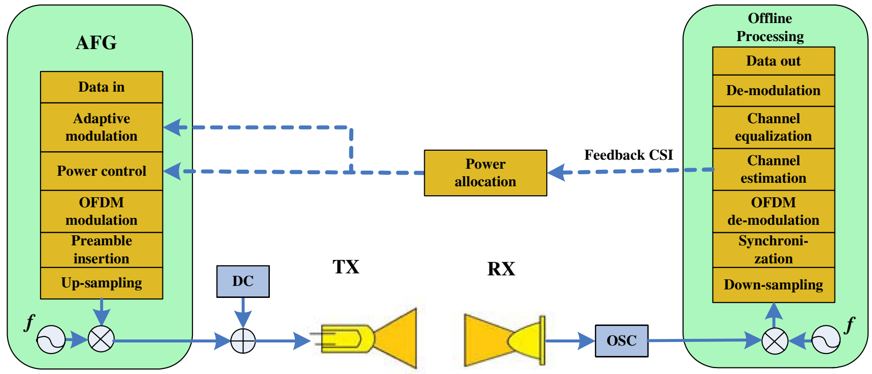

Fig. 1. Block diagram of the proposed adaptive OFDM VLC system (TX: transmitter; RX: receiver).

At the transmitter, a stream of random binary input data is first converted into several parallel data streams, each of which corresponds to a frequency-flat subchannel in the OFDM system. Then power allocated to each subchannel is computed based on the idea of maximizing the channel capacity using the channel state information (CSI), which is estimated at the receiver and fed back to the transmitter. Different modulation orders are determined for each subchannel by the power, CSI, and a pre-set target BER. Then parallel data streams are modulated according to the determined modulation orders. Power control is performed based on the results of power allocation to adjust the transmitted power of the subchannels. OFDM modulation is implemented by inverse fast Fourier transform (IFFT), and a cyclic prefix (CP) is attached to each OFDM symbol to overcome the ISI. An additional OFDM symbol named ‘preamble’ is generated for frame synchronization and inserted in front of the data streams. Finally, OFDM symbols are upsampled and upconverted to a certain carrier.

In the experiment, transmitted signals are generated by an arbitrary function generator (AFG). Direct current (DC) supplied by the AFG is also added to ensure that the transmitted signals are positive. Then the mixed signals are transmitted through an LED in the form of optical power. A commercially available LED (Cree XLamp XP-E) radiating red light is used as the transmitter, whose center wavelength is 620 nm. It generates a luminous flux of about 106 lm at 350 mA of bias current.

At the receiver, the optical signals are focused on the photodiode (PD) and converted into electrical signals. A PD module (Thorlabs PDA10A, 0.45 A/W responsivity at 750 nm) with a 0.8 mm^2 active area and about 150 MHz bandwidth is used as the receiver. The signals are recorded by a commercial high-speed digital oscilloscope (OSC) and then sent for demodulation. The demodulation is performed with offline signal processing, which is the inverse process of the signal modulation at the transmitter. DC is first removed from the signals, and downconverting and downsampling are performed. Frame synchronization is required to detect the starting position of the data streams by the preamble. Then OFDM symbols are demodulated by fast Fourier transform (FFT). CSI is estimated in the frequency domain, which is required for power allocation at the transmitter and channel equalization in the receiver. After channel equalization, ISI that has been induced by channel can be eliminated; meanwhile, further phase synchronization can also be achieved by channel equalization. Demodulation is carried out according to the modulation orders determined by adaptive modulation. Finally, the binary data stream is recovered.

In the proposed adaptive transmission scheme, the spectrum efficiency is maximized by power allocation and adaptive modulation. First, more power is allocated to the subchannels with larger SNR based on the idea of maximizing the channel capacity[16]. It can be formulated as the optimization problem

$$\max_{P(1)\cdots P(N)} \sum_{k=1}^{N} C(k) = \sum_{k=1}^{N} \log\left(1 + \frac{|H(k)|^2 P(k)}{N_0}\right), \qquad (1)$$

subject to

$$\sum_{k=1}^{N} P(k) = N \;\; P(k) \geq 0 \qquad k = 1, \cdots, N, \qquad (2)$$

where k stands for the subchannel index. The channel is divided into N subchannels; that is, each OFDM symbol has N subcarriers. $C(k)$ is the capacity for the kth subcarrier. $H(k)$ is the CSI for the kth subcarrier, and $P(k)$ is the transmitted power for the kth subcarrier. N_0 is the noise power, which is also estimated at the receiver. Here, we assume that the total transmitted power is equal to N.

The water-filling algorithm is used to solve the problem. Employing the Lagrange multiplier method for optimization with an equality constraint in Eq. (2), the power allocated for each subcarrier is obtained as[17]

$$P(k) = \left(\frac{1}{\lambda} - \frac{N_0}{|H(k)|^2}\right)^+ = \begin{cases} \frac{1}{\lambda} - \frac{N_0}{|H(k)|^2}, & \text{if } \frac{1}{\lambda} - \frac{N_0}{|H(k)|^2} \geq 0 \\ 0, & \text{otherwise} \end{cases}, \quad (3)$$

where λ is the Lagrange multiplier. This solution implies that the sums of the power and noise-to-signal ratio (NSR) for each subcarrier must be the same for all subcarriers (i.e., $P(k) + N_0/|H(k)|^2 = 1/\lambda = \text{constant}$), except for the subcarriers that have been assigned no power just because $1/\lambda - N_0/|H(k)|^2 < 0$.

Second, adaptive modulation is applied to achieve maximum channel capacity. Different modulation orders are determined for each subcarrier by a target BER and the received SNR. Since each subchannel can be considered as an additive white Gaussian noise (AWGN) channel, the BER with multilevel quadrature amplitude modulation (M-QAM) modulation is bounded by[18]

$$\text{BER} \leq 0.2 \exp\left(-1.5\frac{\gamma}{M-1}\right), \quad \text{if } M \geq 4, \quad (4)$$

$$\text{BER} \leq 2 \exp\left(-1.5\frac{\gamma}{M-1}\right), \quad \text{if } M < 4, \quad (5)$$

where γ is the received SNR and M stands for the modulation order.

Thus, the modulation order for the kth subcarrier can be obtained if the BER target BER_T is given, which is expressed as

$$M(k) = \left\lfloor 1 - \frac{1.5\gamma(k)}{\log(5\text{BER}_T)} \right\rfloor, \quad \text{if } M \geq 4, \quad (6)$$

$$M(k) = \left\lfloor 1 - \frac{1.5\gamma(k)}{\log(0.5\text{BER}_T)} \right\rfloor, \quad \text{if } M < 4, \quad (7)$$

where $\gamma(k) = P(k)|H(k)|^2/N_0$. The option $\lfloor \cdot \rfloor$ will always round down to the nearest integer since the modulation order should be an integer. Considering that the constellation sizes of the QAM signals must be powers of 2, the modulation orders M^* are determined discretely according to Table 1.

As soon as the modulation orders are determined, the binary data of each subchannel is mapped into QAM signals. Note that the average signal power of different modulation orders should be normalized during the constellation mapping. Then power control is implemented based on the result of power allocation. Factors determined by the power allocation are multiplied by subcarriers to adjust the transmitted power of each subchannel.

The experimental setup for the proposed OFDM-based adaptive VLC system is shown in Fig. 2. In this experiment, a Tektronix AFG3252C was used to generate the transmitted signals. Data were recorded by a commercial high-speed digital OSC (Tektronix MSO4104) with a maximum sampling rate of 5 GSa/s. The signal peak-to-peak voltage was set at 3 V, and the offset was 2.5 V.

The performance of the adaptive OFDM VLC system with different transmission bandwidths was examined. The system parameters configured in the experiment are listed in Table 2.

The normalized amplitude frequency response of the equivalent channel measured by channel estimation is shown in Fig. 3, which includes the frequency responses of the LED, optical channel, and the PD. As can be seen,

Table 1. Determination of Modulation Orders

M	M^*
$M < 2$	0
$2 \leq M < 4$	2
$4 \leq M < 8$	4
$8 \leq M < 16$	8
$16 \leq M < 32$	16
$32 \leq M < 64$	32
$64 \leq M < 128$	64
$128 \leq M < 256$	128
$M > 256$	256

Fig. 2. Experimental setup for the proposed system.

Table 2. Parameter Configuration

Parameters	Details
Bandwidth (MHz)	25/12.5/6.26
Up-converted frequency (MHz)	15/8.75/5.625
Subcarrier number	256
Number of CP	32
Up-sampling rate	4
Distance between transmitter and receiver (cm)	40

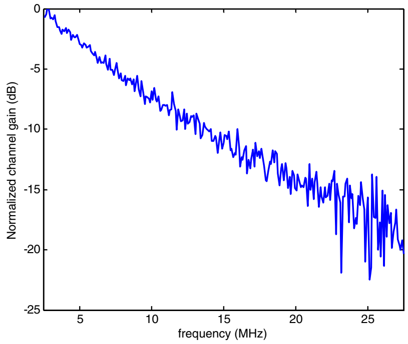

Fig. 3. Normalized amplitude frequency response of the equivalent channel.

the frequency response was strongly attenuated at high frequencies.

The measured spectra of the received signals with three bandwidths are shown in Fig. 4. Different upconverted frequencies were chosen to ensure that the start position of the signal spectra were the same, where the spectrum ranged from 2.5 to 27.5 MHz for the 25 MHz bandwidth case, from 2.5 to 15 MHz for the 12.5 MHz bandwidth case, and from 2.5 to 8.75 MHz for the 6.25 MHz bandwidth case. The results show that the spectrum with a broader bandwidth experienced more severe fading since the channel was strongly attenuated at high frequencies. The power and bit allocation results in the condition of $\text{BER}_T = 0.001$ are depicted in Figs. 5 and 6, respectively. The SNR of each subcarrier is also given in Fig. 5. In order to make the experimental results comparable, the total transmitted power for all the experiments was kept the same. More power was allocated to those subcarriers with higher received SNR, which was determined by the CSI and the noise power. As a result, the transmitted power of different subcarriers appeared to change less for the narrow bandwidth case, as shown in Fig. 5. Correspondingly, higher modulation orders tended to be assigned to the subcarriers for the narrow bandwidth case due to their high SNR, as shown in Fig. 6.

Spectrum efficiency performance comparisons between VLC systems with and without an adaptive transmission

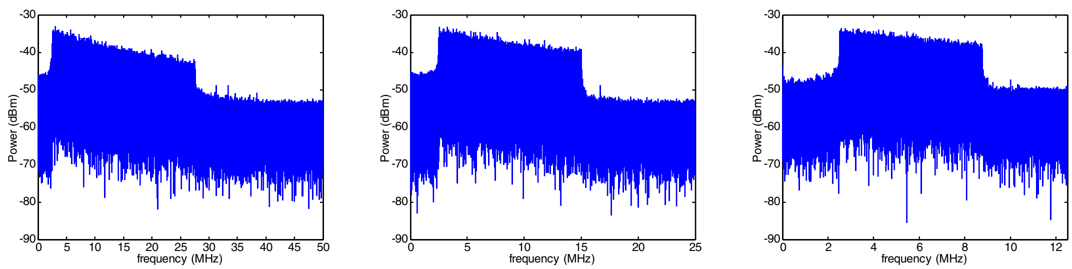

Fig. 4. Measured electrical spectra of the received signals for the (a) 25 MHz case, (b) 12.5 MHz case, and (c) 6.25 MHz case.

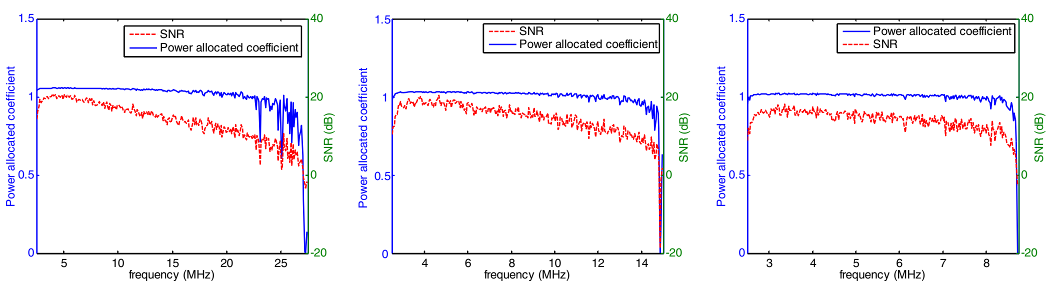

Fig. 5. SNR and power allocated results for the (a) 25 MHz case, (b) 12.5 MHz case, and (c) 6.25 MHz case.

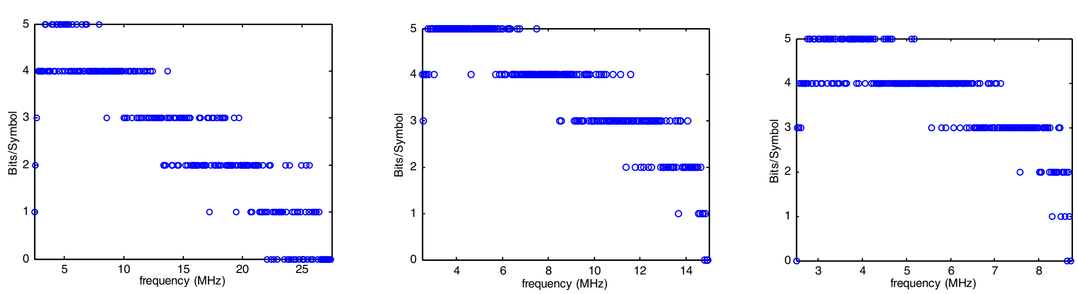

Fig. 6. Bits allocated results ($\text{BER}_T = 0.001$) for the (a) 25 MHz case, (b) 12.5 MHz case, and (c) 6.25 MHz case.

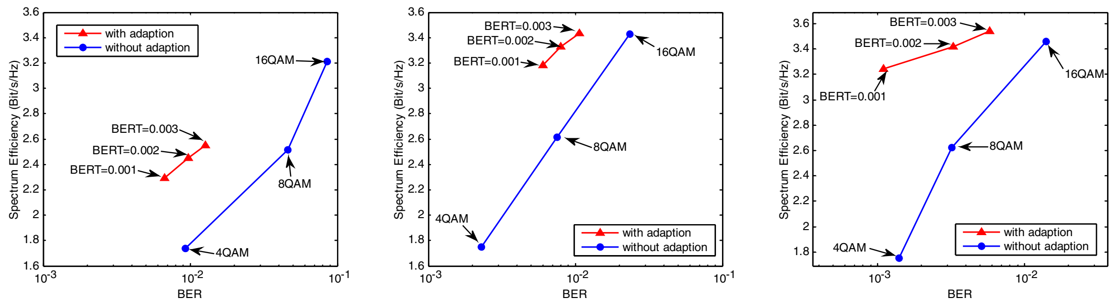

Fig. 7. BER versus spectrum efficiency with and without an adaptive transmission scheme for the (a) 25 MHz case, (b) 12.5 MHz case, and (c) 6.25 MHz case.

scheme are shown in Figs. 7(a), 7(b), and 7(c), which represent the experimental results for different bandwidths. In the experiment, the transmitted data rates of the 25 MHz bandwidth case are 57.4, 61.9, and 64.6 Mbit/s, respectively, for target BERs equal to 0.001, 0.002, and 0.003. For the 12.5 MHz bandwidth case, the data rates are 40.0, 42.0, 43.4 Mbit/s, and for the 6.25 MHz bandwidth case, the data rates are 20.3, 21.5, and 22.3 Mbit/s. In Fig. 7, blue curves stand for the BER versus spectrum efficiency for VLC systems without an adaptive transmission. Each point represents the performance of a certain modulation type, plotted with the BER on the horizontal axis and the spectrum efficiency on the vertical. As can be seen, the BER performance decreases when the modulation orders are increased; however, the performance of the spectrum efficiency improves. The red curves depict the BER versus the spectrum efficiency for VLC systems with an adaptive transmission. Each point represents the performance based on a certain target BER, plotted with the BER on the horizontal axis and the spectrum efficiency on the vertical. Obviously, when increasing the BER target, the adaptive modulation orders also increase. As a result, the spectrum efficiency is also improved. The experiment results also show that the adaptive transmission scheme can improve the spectrum efficiency significantly when the BER level is kept the same. It was also found that spectrum efficiency is highest for the 6.25 MHz bandwidth case. This is because the received SNR was higher in the narrow bandwidth case and the higher modulation orders are determined in the adaptive modulation procedure. Furthermore, since the channel estimated error and the noise power estimated error are unavoidable, there are gaps between the real system BER and the target BER.

In conclusion, we propose and experimentally demonstrate a simple VLC system by combining the adaptive transmission technique with OFDM. In the experiment, the performance of the adaptive OFDM VLC system is studied and compared with three different transmission bandwidths. Experimental results show that spectrum efficiency can be greatly increased through the application of an adaptive transmission scheme. Experimental results also show that the spectrum efficiency performance is higher with a narrow bandwidth.

This work was supported by the National Natural Science Foundation of China (No. 61501296) and the Key Laboratory for Information Science of Electromagnetic Waves (No. EMW201507).

References

1. L. Hanzo, H. Haas, S. Imre, D. O'Brien, M. Rupp, and L. Gyongyosi, Proc. IEEE **100**, 1853 (2012).
2. A. Jovicic, J. Li, and T. Richardson, IEEE Commun. Mag. **51**, 26 (2013).
3. L. Grobe, A. Paraskevopoulos, J. Hilt, D. Schulz, F. Lassak, F. Hartlieb, C. Kottke, V. Jungnickel, and K. D. Langer, IEEE Commun. Mag. **51**, 60 (2013).
4. A. Sevincer, A. Bhattarai, M. Bilgi, M. Yuksel, and N. Pala, IEEE Commun. Surv. Tutorials **15**, 1620 (2013).
5. N. Chi, Y. Wang, Y. Wang, X. Huang, and X. Lu, Chin. Opt. Lett. **12**, 010605 (2014).
6. R. Li, Y. Wang, C. Tang, Y. Wang, H. Shang, and N. Chi, Chin. Opt. Lett. **11**, 080605 (2013).
7. H. Elgala, R. Mesleh, and H. Haas, IEEE Trans. Consum. Electron. **55**, 1127 (2009).
8. A. M. Khalid, G. Cossu, R. Corsini, P. Choudhury, and E. Ciaramella, IEEE Photon. J. **4**, 1465 (2012).
9. R. Zhang, J. Li, Z. Huang, and Y. Ji, Chin. Opt. Lett. **13**, 072302 (2015).
10. Y. Q. Wang, N. Chi, Y. G. Wang, R. L. Li, X. X. Huang, C. Yang, and Z. R. Zhang, Opt. Express **21**, 27558 (2013).
11. L. Wu, Z. C. Zhang, J. Dang, and H. P. Liu, J. Lightwave Technol. **33**, 117 (2015).
12. K. H. Park, Y. C. Ko, and M. S. Alouini, IEEE Trans. Commun. **61**, 1535 (2013).
13. C. Gong, S. B. Li, Q. Gao, and Z. Y. Xu, IEEE Trans. Signal Process. **63**, 4245 (2015).
14. C. W. Chow, C. H. Yeh, Y. F. Liu, P. Y. Huang, and Y. Liu, Opt. Comm. **292**, 49 (2013).
15. C. H. Yeh, C. W. Chow, H. Y. Chen, J. Chen, and Y. L. Liu, Opt. Express **22**, 9783 (2014).
16. V. Asghari and S. Aissa, IEEE Trans. Wireless Commun. **9**, 3272 (2010).
17. T. David and P. Viswanath, *Fundamentals of Wireless Communication* (Cambridge University Press, 2005).
18. J. A. Goldsmith and S. G. Chua, IEEE Trans. Commun. **45**, 1218 (1997).